13. Source apportionment of freeway-side PM2.5 using ATOFMS

i. Introduction

Recent studies have shown that vehicle emissions are a major source of pollution in urban areas (399-403,434,435). With an ever growing concern over the health effects associated with vehicle emissions, a goal of major federal and state agencies is to set regulations which lead to a reduction in these pollutants (280,404,405). The ability to apportion gasoline powered light duty vehicles (LDV), heavy duty diesel vehicles (HDDV), and other combustion emissions in ambient aerosols will allow city and state agencies to channel their efforts and resources into targeting the major polluters (LDV, HDDV, and other combustion sources) in their area. Distinguishing between LDV and HDDV exhaust aerosols may represent the greatest challenge (compared to other combustion sources) due to the similar chemical characteristics of the PM in their emissions, which result from their similar fuel and oil composition (403,436-440).

The purpose of this work is to test whether aerosol mass spectral source signatures acquired from ATOFMS source characterization studies, including vehicle dynamometer studies, can be used to apportion ambient aerosols in a freeway-side study. A freeway-side location was chosen in a coastal area because this location should be dominated by particles from fresh vehicle exhaust emissions and should display a relatively low concentration of aged or transformed particles. The background particles are expected to be mostly sea salt since this is a coastal region. The steps involved in data quality assurance will be discussed as well as how particle size measurements and gas phase instrumentation can be incorporated for aerosol source apportionment.

ii. Experimental

The experimental setup used for this study has been described in Chapter 4 (441). The study was conducted from July 21 to August 25, 2004 at two sites. First, a "clean" upwind site was stationed at the Prather Laboratory in Urey Hall at the University of California, San Diego (UCSD) with the goal of determining the signatures of background ambient aerosols (GPS position 32°52'31.66"N 117°14'28.64"W). This site is relatively close to the ocean (within 950 meters) so the prevailing winds (from the west) should introduce little-to-no fresh source emissions. This site housed a standard inlet ATOFMS instrument (127) along with an aerodynamic particle sizer (APS) (TSI Model 3321 – Minnesota) and a scanning mobility particle sizer (SMPS) (TSI Model 3936L10 – Minnesota). The second site was located at a trailer stationed in a

Table 16: List of Instrumentation used at the freeway and upwind sampling sites.

Instrument	Make & Model	Measurement	Units	Sample Resolution	Site	Sampling Period
Ultrafine Aerosol Time-of-Flight Mass Spectrometer (UF-ATOFMS)		size range: 50–300 nm		real-time	Freeway	Jul 21 to Aug 25, 2004
Standard Aerosol Time-of-Flight Mass Spectrometer (ATOFMS) 1		size range: 200–3000 nm		real-time	Freeway	Jul 21 to Aug 25, 2004
Standard Aerosol Time-of-Flight Mass Spectrometer (ATOFMS) 2		size range: 200–3000nm		real-time	Upwind	Jul 21 to Aug 2, 2004
					Freeway	Aug 10 to Aug 25, 2004
Aerodynamic Particle Sizer (APS) 1	TSI Model 3321	particle number conc. (0.5–20µm)	#/cm^3	5 min	Freeway	Jul 21 to Aug 25, 2004
Aerodynamic Particle Sizer (APS) 2	TSI Model 3321	particle number conc. (0.5–20µm)	#/cm^3	5 min	Upwind	Jul 21 to Aug 2, 2004
Scanning Mobility Particle Sizer (SMPS) 1	TSI Model 3936L10	particle number conc. (10–500nm)	#/cm^3	5 min	Freeway	Jul 21 to Aug 25, 2004
Scanning Mobility Particle Sizer (SMPS) 2	TSI Model 3936L10	particle number conc. (10–500nm)	#/cm^3	5 min	Upwind	Jul 21 to Aug 2, 2004
Aethalometer	Magee Scientific 'Spectrum' AE-3 Series	optical absorption cross-section per unit mass	µm/m^3	5 min	Freeway	Jul 21 to Aug 25, 2004
Nephelometer	Radiance Model M903	light scattering coefficient (bscat)	km^{-1}	5 min	Freeway	Jul 21 to Jul 22 & Jul 25 to Aug 25, 2004
Photoelectric Aerosol Sensor (PAS)	EcoChem Model 2000	concentration of total particle-bound PAH	ng/m^3	5 min	Freeway	Jul 30 to Aug 25, 2004
Tapered Element Oscillating Microbalance (TEOM)	Rupprecht & Patashnick (R & P) Series 1400a	mass concentration ($PM_{2.5}$)	µg/m^3	30 min	Freeway	Jul 21 to Aug 25, 2004
Chemiluminescence NO-NO2-NOx Analyzer	Thermo Environmental Instruments (TEI) Model 42C	NO & NOx concentration levels	ppb	1 min	Freeway	Aug 5 to Aug 25, 2004
CO Analyzer	Advanced Pollution Instrumentation (API) Model M300	CO concentration levels	ppm	5 min	Freeway	Jul 30 to Aug 10 & Aug 13 to Aug 25, 2004
Webcam	Creative Model PD1001	traffic video surveillance		1 sec	Freeway	Jul 21 to Aug 25, 2004

low-use parking lot (particularly during the summer) on the UCSD campus directly adjacent to the I-5 freeway (GPS position 32°52'49.74"N 117°13'40.95"W) with the sampling line within 10 meters of the freeway. The trailer housed a suite of instruments including an ATOFMS and UF-ATOFMS (417). A detailed summary of the instrumentation operated at both sites is provided in **Table 16**. Dr. Michael Kleeman's research group (UC Davis) also sampled PM at both sites with micro orifice uniform deposit impactors (MOUDI's), Anderson Impactors, an APS, and an SMPS. The Kleeman group sampled from July 21 - August 1. Their measurements focused on obtaining size-resolved concentrations of organic and metal tracers to be used for conventional source apportionment. Ultimately, when their results become available, a comparison will be made between the ATOFMS apportionment results and the impactor-

based predictions. Meteorological stations were operated on each side of the freeway for complete wind trajectory information.

iii. Results and Discussion

a. Quality Assurance of ATOFMS Data

Data from the three ATOFMS instruments as well as all peripheral instruments were loaded into a database that allows for direct comparison of the temporal trends of gas phase, particle phase, and meteorological data. Before beginning data analysis of the ATOFMS particle types, quality assurance (QA) graphs were prepared for all three instruments over the relevant size ranges of the study. The purpose of these graphs is to examine whether any anomalies occurred during sampling that would result in improper interpretation of the acquired data.

A question that often arises with ATOFMS data concerns whether any chemical biases are leading to particles being "missed" in the LDI analysis step. In order to check for the presence of chemical biases, temporal plots are compared of the number of particles which scatter light to the number of particles which scatter light and produce a mass spectrum. If there is a chemical bias, where a particular type is being "missed", it will show up as lots of "scatters" with very few "scatters + mass spectra" (442). These plots were made for all three ATOFMS instruments over multiple size ranges for the full duration of the study. An example of this type of plot is shown in **Figure 94A** for the UF-ATOFMS. As can be seen, there are no major deviations between the scatters and scatters + mass spectra over the time of the study, indicating that there are major period with missed particle types. It is important to note that the smallest sized particles have the highest probability of showing a chemical bias since smaller particles are more "pure" (i.e. less chemically complex). In the freeway study, there was no major evidence of any particle types being missed by the ATOFMS in any of the size ranges examined (50 – 3000 nm). This is not surprising since the particle emissions from vehicles strongly absorb the ultraviolet light at 266 nm used for the laser desorption/ionization process with the ATOFMS. It should also be noted that all temporal plots for ATOFMS data shown in this manuscript show unscaled ATOFMS number concentrations. As will be shown, the unscaled temporal trends of the ATOFMS track the peripheral instruments without scaling; the main reason for scaling is to obtain atmospherically representative concentrations that can be directly compared to results from other studies.

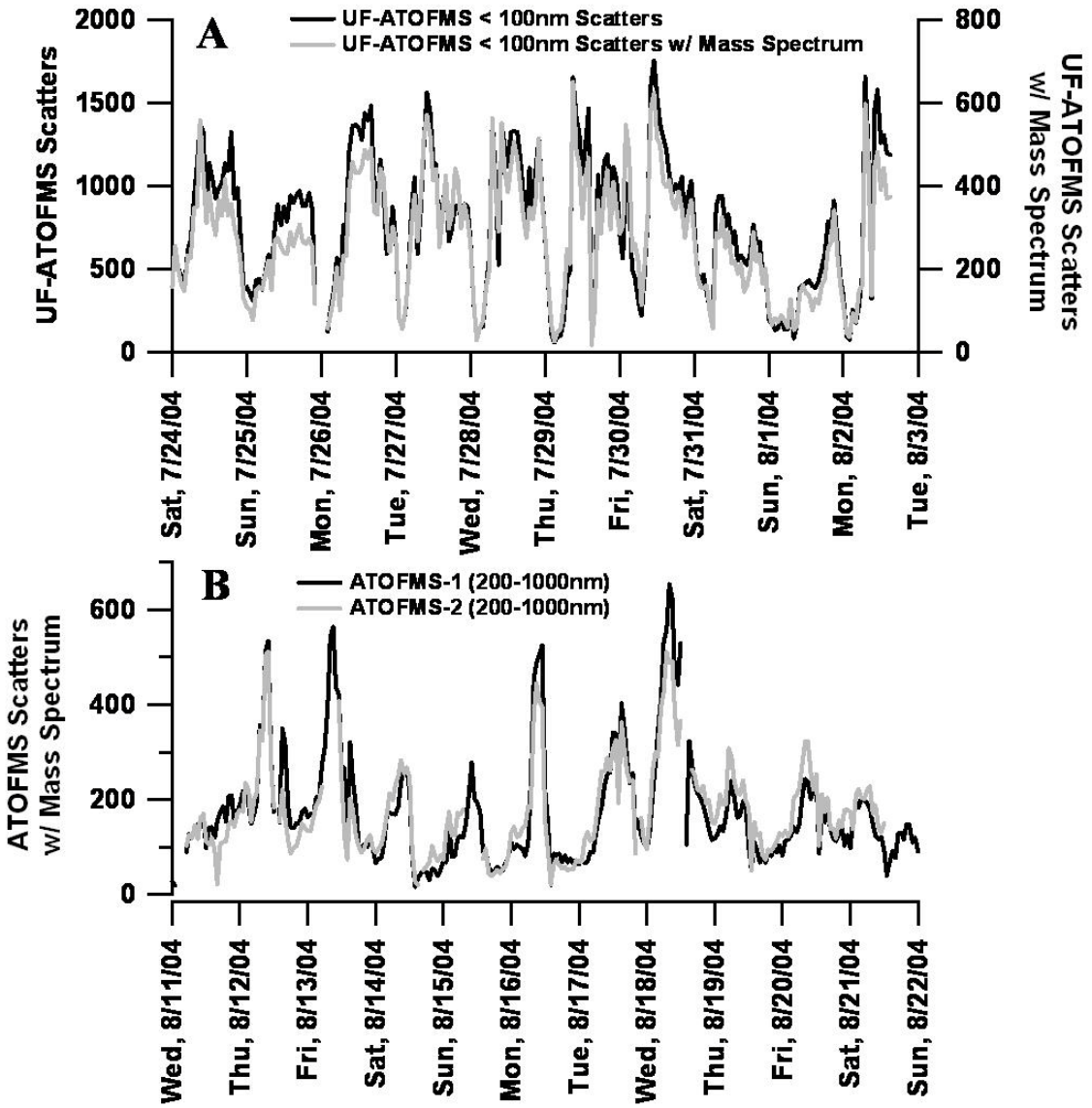

Figure 94: A) QA plot of UF-ATOFMS particle scatters vs. particles scattered that produced a mass spectrum to determine if there are any chemical biases or particle types being missed. B) Comparison of the two standard inlet ATOFMS instruments particle detections when running side-by-side at the freeway site. Plots are in one hour resolution.

As part of the QA process, it is also important to compare the temporal trends for the two standard inlet ATOFMS instruments when they were sampling side-by-side for the last part of the study near the freeway. **Figure 94B** shows this comparison, demonstrating how when the instruments were located at the same site almost identical trends in particle counts are obtained, demonstrating the reproducibility of the ATOFMS systems.

b. Comparison with standard particle counts

Comparing the ATOFMS size distribution measurements with those from other particle size measuring instruments is an additional method for determining whether the trends observed with the ATOFMS reflect ambient particle concentrations. **Figure 95A** shows a comparison of the SMPS against the UF-ATOFMS for sub-100 nm particle counts. Despite being on different absolute scales, it is evident that the basic temporal trends measured by these two instruments track one another quite well (R^2 = 0.60), providing additional validation of the ATOFMS temporal trends. In general, the ultrafine counts increased during periods when the winds were blowing from the west directly from the freeway to the sampling site. At night, the wind speeds typically became quite low (< 1.0 m/s), the traffic was reduced, and the ultrafine particle counts were at their lowest. This pattern was repeated each day over the entire study.

The two standard inlet ATOFMS systems measured particles in the larger size modes (200 – 3000 nm). **Figure 95B** shows a comparison of the ATOFMS by the freeway with the APS for submicron counts. The APS only samples particles down to 500 nm so a slightly different size range is covered. The standard ATOFMS detected

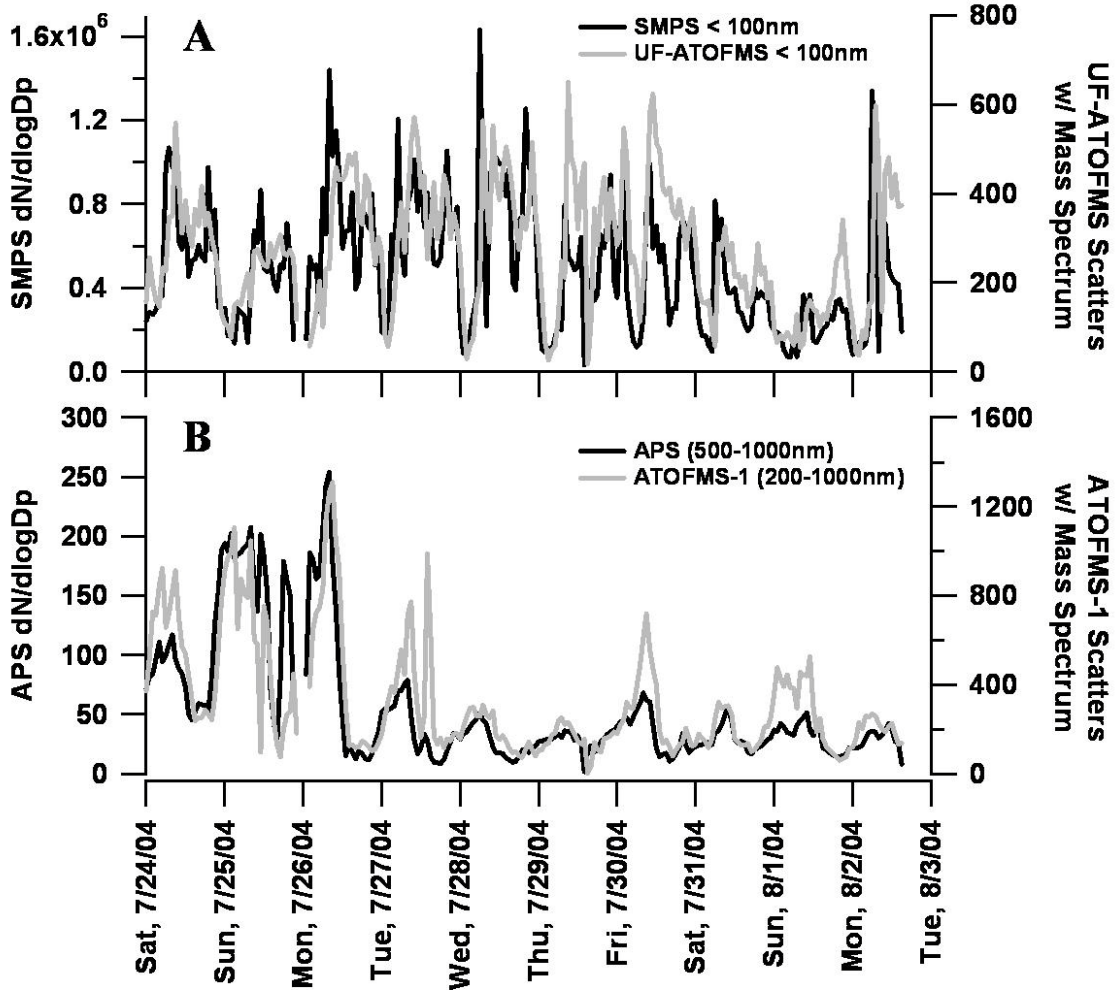

Figure 95: A) Comparison of sub-100 nm particle counts with the SMPS to sub-100 nm particles detected (that produced mass spectra) with the UF-ATOFMS at the freeway site. B) Comparison of fine mode particles (500 – 1000 nm) with the APS to fine mode particles (200 – 1000 nm)

detected (that produced mass spectra) with the standard inlet ATOFMS at the freeway site. Plots are in one hour resolution.

very few particles below 300 nm due to limitations in the transmission efficiency of the inlet. The important thing to note about this comparison is how strongly correlated the trends are ($R^2 = 0.70$), offering further credence to the temporal variations measured with the ATOFMS. **Figure 95A-B** shows the ATOFMS instruments tracking particle number concentrations measured using traditional particle sizing instruments over a broad range of sizes. This validation step is extremely important to future studies probing the temporal variability of different source contributions to the various ambient particles sampled by ATOFMS.

c. Comparison of particle phase and gas phase data

It is interesting to compare the UF-ATOFMS measurements with gas phase measurements. **Figure 96A** and **Figure 96B** show a comparison of gas phase CO and NO_x concentration measurements versus UF-ATOFMS counts, indicating time periods when fresh emissions were impacting the sampling site. **Figure 96C** shows an expanded view of each gas phase species plotted over a larger time span. Typically it is expected that time periods where UF particles and CO peak may be related to LDV exhaust periods (426), whereas increases in NO_x concentrations could be more indicative of HDDV emissions (425-427). When comparing the trends between CO and NO_x emissions though, their trends tracked each other very closely ($R^2 = 0.71$). Since the trends are so similar, one cannot generalize that the CO is for LDVs and the NO_x represents HDDVs in this case. More likely, these trends follow so closely because they are tracking both the trends in traffic as well as wind patterns. The CO and NO_x values presented here (where the CO emissions are

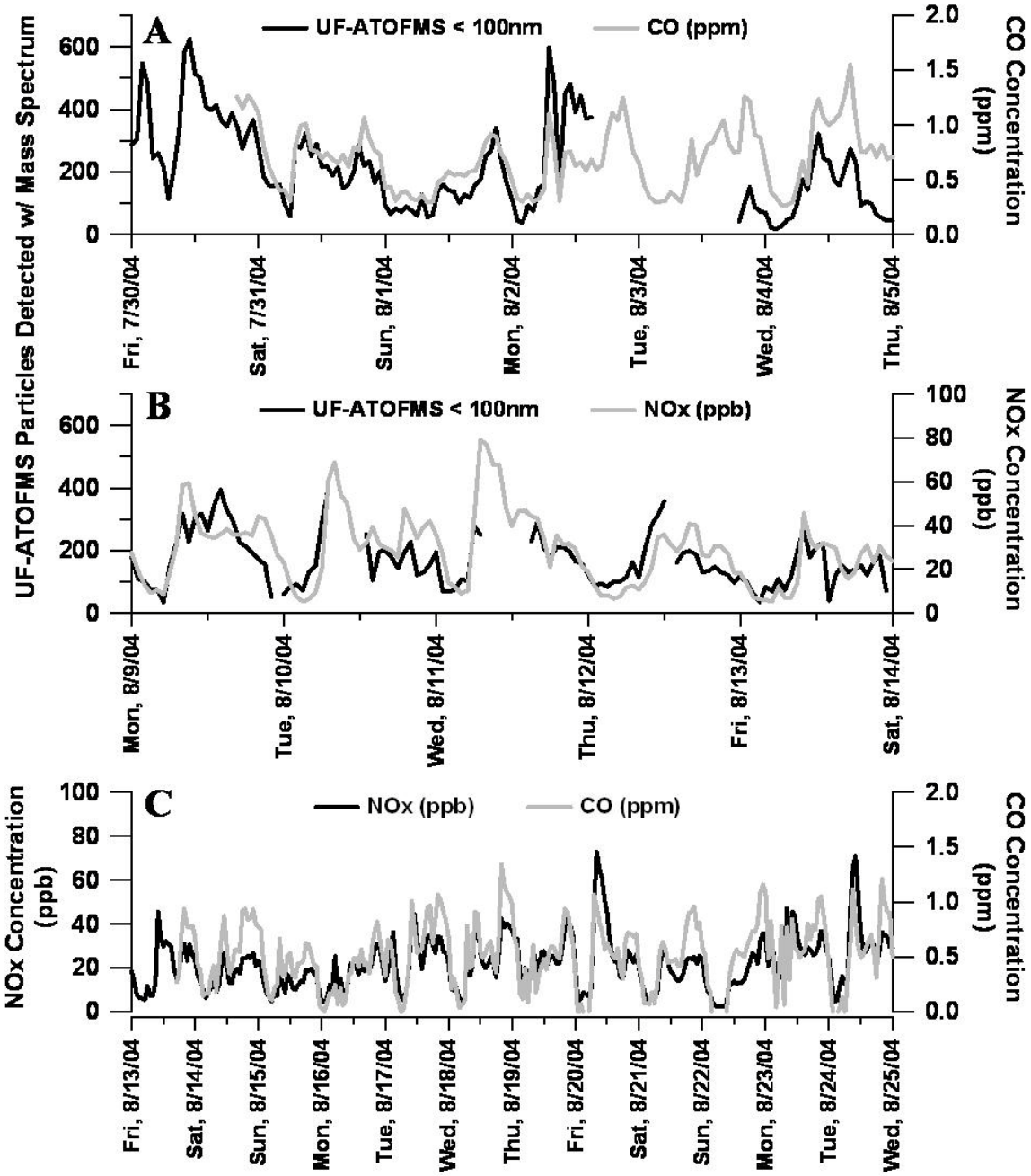

Figure 96: A) Comparison of sub-100 nm UF-ATOFMS particles detected that produced mass spectra with CO measurements. B) Comparison of sub-100 nm UF-ATOFMS particles detected that produced mass spectra with NO_x measurements. C) Comparison of CO and NO_x measurements at the freeway site. Plots are in one hour resolution.

continuously higher than the NO_x emissions) are consistent with previous findings for areas with similar traffic conditions (426,443).

d. Comparison of temporal trends from peripheral instruments

Analysis of gas phase species such as NO_x and CO coupled with aethalometer data can provide insight into the time periods when vehicle exhaust plumes were impacting the sampling site. There is some speculation as to whether this combination of instruments coupled with ultrafine size distribution measurements made with an SMPS can be used to identify HDDV impacted events (408,409,444-446). **Figure 97A** shows a comparison of the aethalometer and NO_x measurements made over a time period when all instruments were operational. In general, the trends observed between the ultrafine particle concentrations (<100 nm), CO, aethalometer, and NO_x measurements tracked each other, following peak wind speeds, which occurred mostly during daytime hours. Likewise, in **Figure 97B**, the data from the nephelometer (which detects light scattering particles) has similar trends as the aethalometer. This correlation is a strong indication that the local winds control when the particles reach the sampling site.

By comparing the aethalometer and NO_x concentrations, one can see the trends track extremely well. In addition, one can see increases during weekdays versus weekends as has been reported in previous studies (444,445,447). This has been attributed to a relative increase in HDDV traffic during the week in Chapter 4. However, based on traffic count data, in addition to fewer HDDVs being on the road on weekends, there are also fewer LDVs

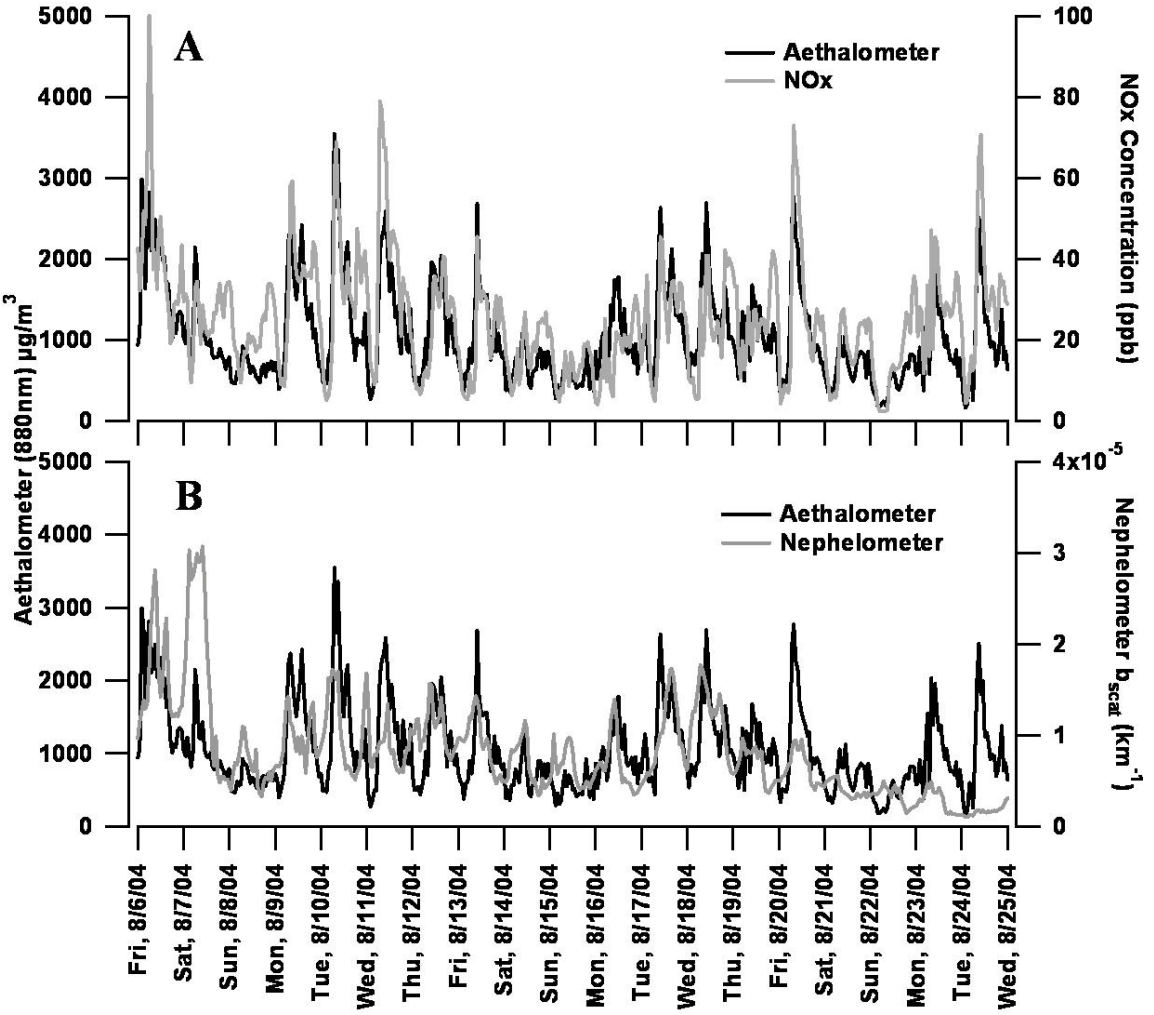

Figure 97: A) Comparison of aethalometer and NO_x measurements at the freeway site. B) Comparison of aethalometer and nephelometer measurements at the freeway site. Plots are in one hour resolution.

overall (441). Therefore, the traffic flow is lower on this stretch of freeway during the weekends compared to the weekdays.

e. Upwind/Downwind Sampling

A major goal of the freeway study involved determining the contributions of vehicle emissions to ambient air near a major freeway. As previously described, an upwind sampling site was established so a comparison could be made between source contributions at a freeway-impacted site and a background (upwind) site. In addition to composition measurements being made with the ATOFMS and filters (Kleeman, UC-Davis), size distribution measurements were made using an APS and SMPS at both locations.

Figure 98A shows the APS and SMPS concentrations for the period between Jul. 24 and Aug. 3, 2004 at the freeway sampling site. **Figure 98B** shows the same data for the upwind sampling site. As can be seen, there is a constant band of particles with sizes

from 250 – 800 nm at the two locations, suggesting a strong regional contribution to the ambient PM levels at both sites. It is important to note that the wind was blowing from the upwind site (onshore) towards the freeway site during daytime hours when the concentrations show maxima at both locations. This figure shows that the concentrations of accumulation mode particles above 200 nm at the upwind/background site were not always lower than those at the freeway site as one would expect if the freeway was the major source of PM in this area.

The ultrafine mode and low size end of the accumulation mode (50 – 300 nm) show higher concentrations at the freeway location (**Figure 98A**), suggesting fresh

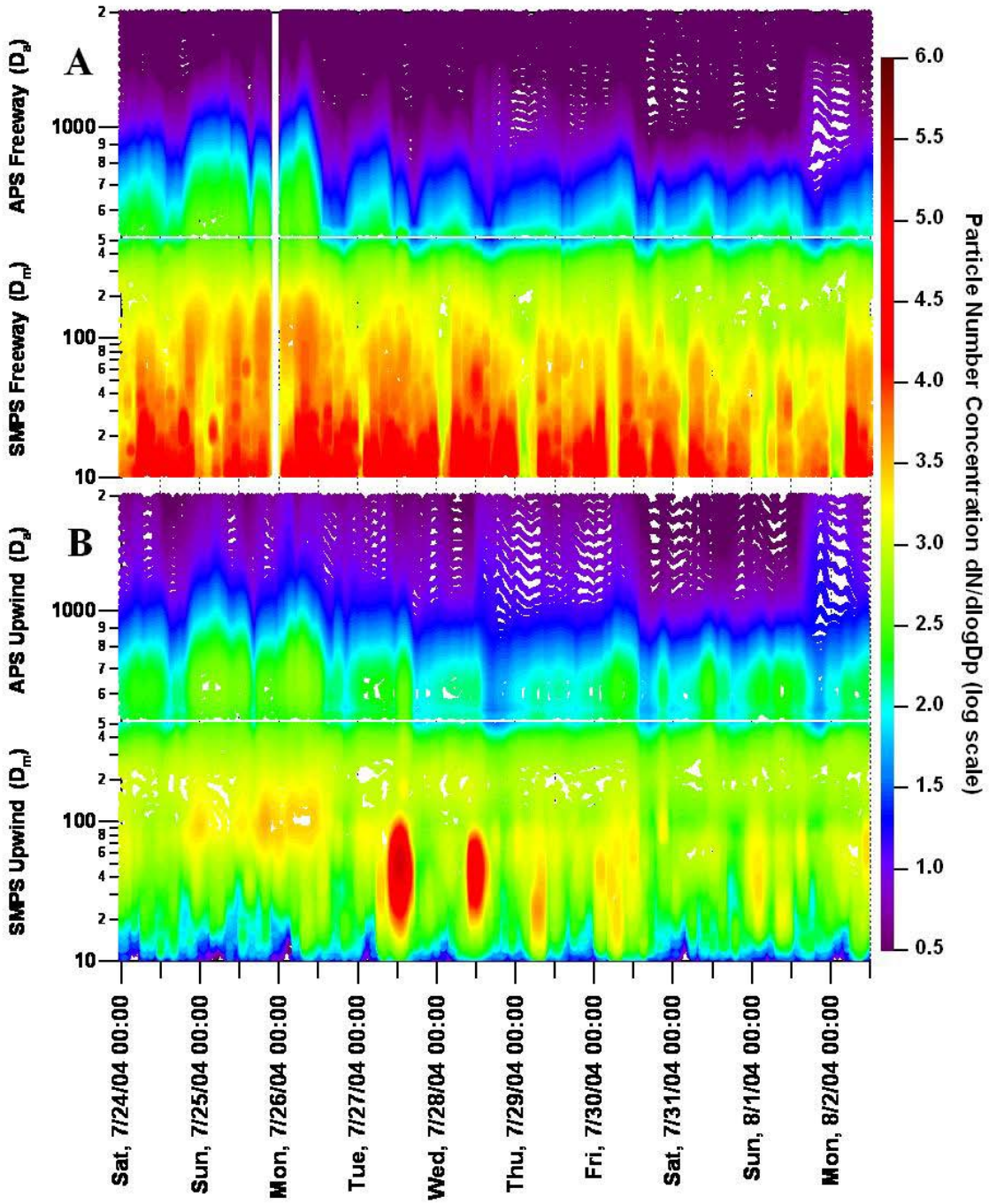

Figure 98: A) SMPS and APS particle number concentrations at the freeway site from. B) SMPS and APS particle number concentrations at the upwind sampling site. Both plots are shown from Jul. 24 to Aug. 3, 2004 in order to directly compare the two sites. The data is shown in log scale.

vehicle emissions from the freeway are contributing to particles in the 50 – 300 nm size range. However, it is interesting to note that on July 27 and 28, at around noon, significantly higher ultrafine and accumulation mode concentrations are observed at the upwind lab site indicating contributions from a local source. The standard instrument (ATOFMS-2) was sampling at the upwind location during this period. An examination

of the single particle composition revealed a unique single particle signature that has been detected as a major particle type in meat cooking emissions in previous meat cooking studies conducted in our laboratory (448). A large potential source of PM on the UCSD campus near the sampling site is a cafeteria where food is grilled. The peak in emissions corresponds to the period of the day when the most people eat at this establishment. Notably, a meat cooking aroma is often detected at the upwind site.

On July 29 and 30, ultrafine concentrations at the upwind site peaked at approximately 6:00 am (**Figure 98B**) and most likely came from traffic on a local road that borders the UCSD campus located close to the upwind site (about 300 m away) which is highly traveled at this hour of the day. In general, ultrafine particle concentrations show the highest spatial variability and represent ideal markers for local source inputs, as they spike only near the emission source. The ultrafine particles are also the most straightforward to identify and apportion since they have undergone very little aging and thus their signatures closely resemble the source (in this case dynamometer testing) signatures.

As shown in **Figure 98**, regional background PM concentrations made significant contributions to the accumulation mode. **Figure 99** compares the size distributions of the ATOFMS instruments [upwind (5.6A) and freeway (5.6B,C)] for the same time period as

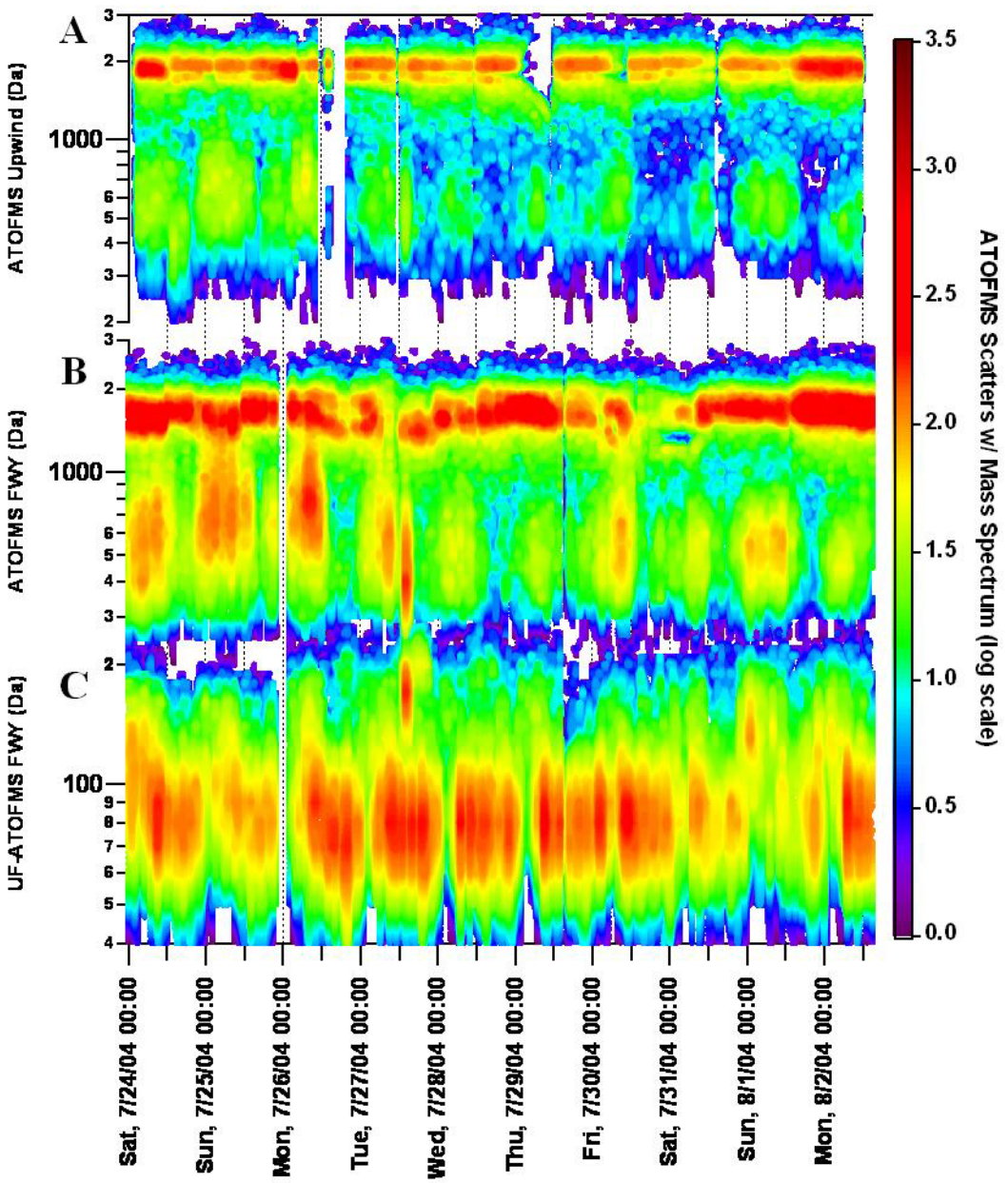

Figure 99: Particle size distribution data of: A) Standard inlet ATOFMS at the upwind sampling site. B) Standard inlet ATOFMS at the freeway sampling site. C) UF-ATOFMS at the freeway site. The particle size data shown is only for particles that were detected that produced a mass spectrum with the particular ATOFMS instrument. The data shown is from Jul. 24 to Aug. 3, 2004 in order to compare the two sites and to the APS and SMPS data shown in Figure 98.

the comparison of APS and SMPS data compared in **Figure 98**. One can see that the accumulation mode size distributions show very similar trends between the upwind and freeway sites. While the freeway site shows higher concentrations in the accumulation mode, the upwind site shows peaks at the same times. The difference in concentrations may be due to the topography of the area. Since the freeway site is located in a lower,

valley-like area, the background aerosols may be more prevalent at this site than at the upwind site which is closer to the coast and at a higher elevation. Evident in this figure is a relatively high PM concentration in the accumulation mode from July 24-27. It can also be seen that the accumulation mode peaks at nighttime and early morning hours, which corresponds to when the local wind speeds are at their lowest levels. This suggests that the accumulation mode particles are either due to smaller particles growing via condensation and/or agglomeration or from background particles at higher altitude settling to ground level. The latter of these scenarios is the most likely because of specific particle types detected that are unique to these time periods.

Due to these accumulation mode background contributions, other particle types were detected during this study that did not match to the vehicle dynamometer signatures. **Figure 100 (A,B)** shows the mass spectra for two such particle types: vanadium and elemental carbon (EC). These particle types peaked during the first few days of the study (July 24-27) in the accumulation mode at both sites usually when the local winds were low, likely indicating a regional contribution. The temporal trends for the vanadium and EC particle types are shown in **Figure 100 (C,D)**. HYSPLIT model (449) 24-hour back trajectories during these peak times show the winds at 500 m coming (southward) down along the California coastline, passing directly over the major shipping

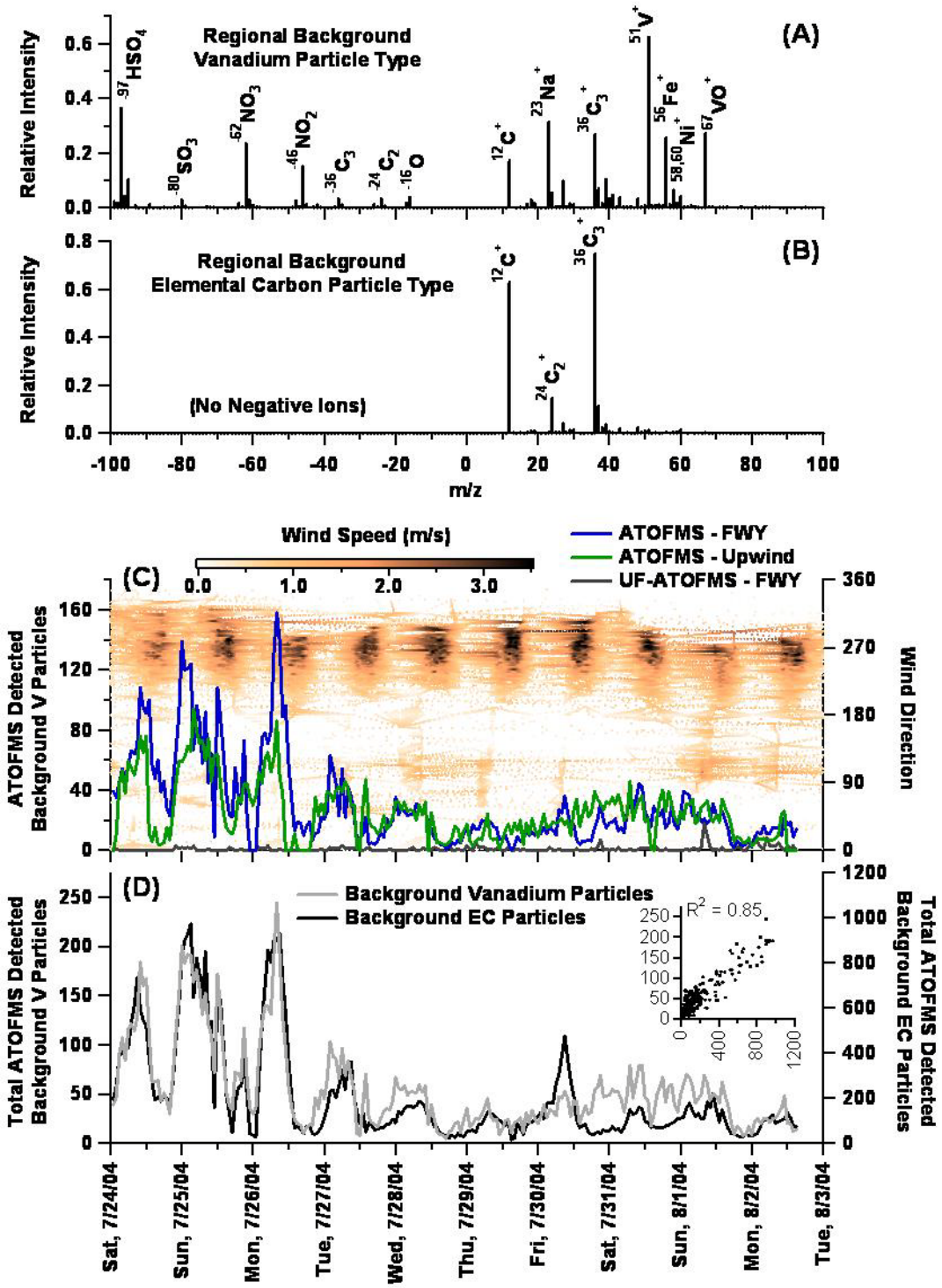

Figure 100: Positive and negative ion mass spectra for the regional background (A) vanadium and (B) EC particle types. (C) The temporal trends of the vanadium particle type detected with all three ATOFMS instruments compared to wind data. (D) Temporal trends (and correlation) of total background vanadium particles versus the total background EC particles for the three ATOFMS instruments.

ports in Long Beach and San Pedro. The HYSPLIT model back-trajectories are shown in **Figure 101**. When comparing the temporal trends of the vanadium & EC particles to the HYSPLIT back trajectories, it can be seen that largest peaks (7/24-7/26) occur when the nighttime wind trajectories are strong and coming straight down the southern California coast from the Los Angeles area. The days with smaller peaks occur when the nighttime trajectories are either not as strong, or are coming into the sampling site from out over the ocean.

Oil combustion has been shown to be the primary source for atmospheric vanadium aerosols (168,291,450,451). Vanadium particles have also been shown to come from vehicles, dust, and industrial sources (418,452,453). The correlation between V, Fe, and Ni associated with this type (as shown in **Figure 100A**) agree with findings by Xie et al. 2006 for ship oil combustion emissions (168). It is interesting to compare the temporal trend for these V-particles in the accumulation mode versus the ultrafine mode. On August 1, the number concentration of these particles shows a spike with the UF-ATOFMS that is not apparent in the accumulation mode, mostly likely indicating a local source. The temporal trends for the background vanadium and EC type, as well as the correlation between EC and V particle types, are shown in **Figure 100D**. As can be seen, the EC and vanadium trends track each other very strongly (R^2 = 0.85), especially from 7/24 to 7/30, with only minor variations occurring between 7/30 and 8/1. This correlation is an indication that the EC and V particle types are transported together and are likely from the same source. The relationship between these types of vanadium and elemental carbon particles and the use

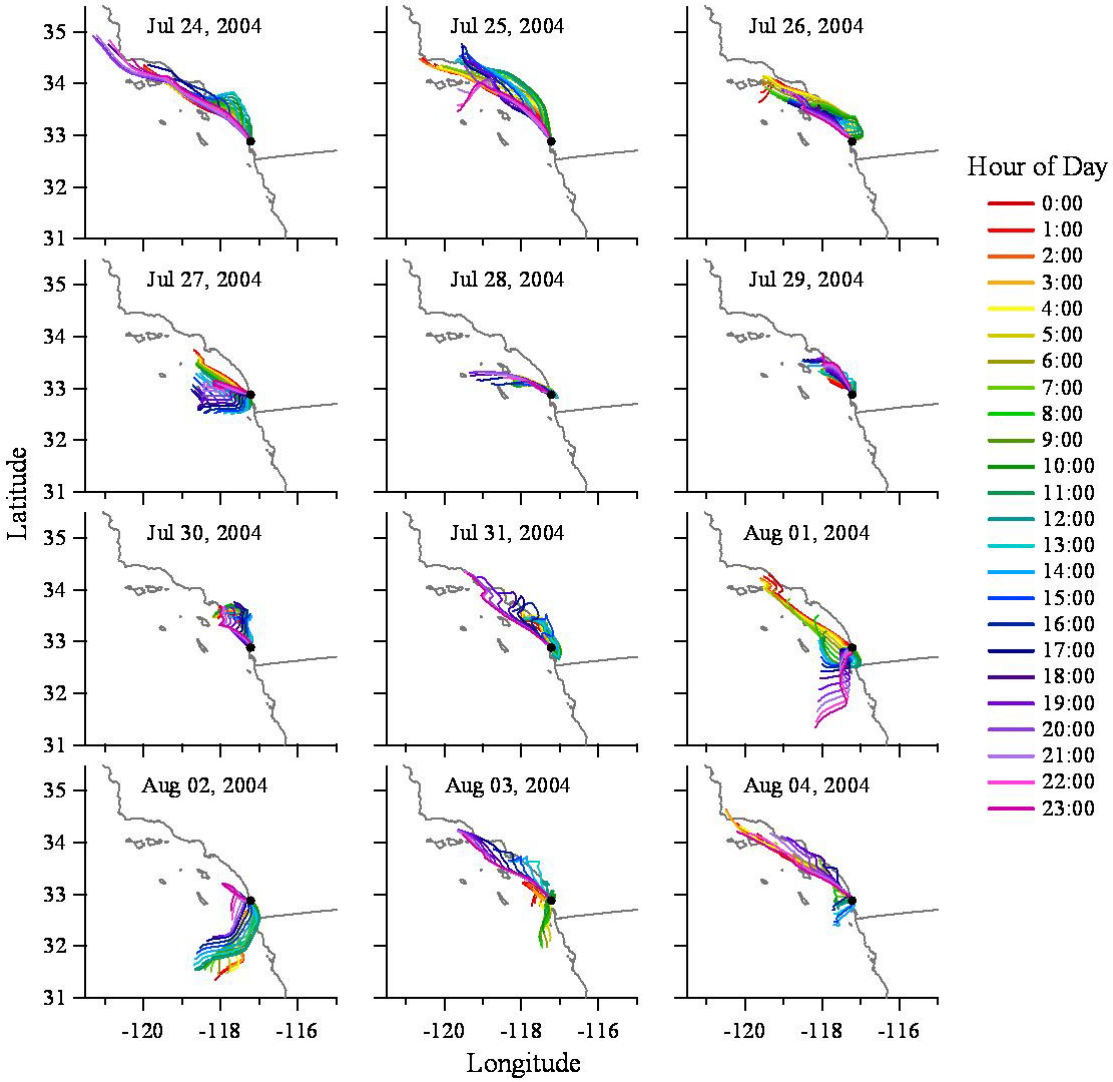

Figure 101: Hourly HYSPLIT model 24-hour back trajectories at 500 m for each day at the freeway study site.

of these signatures for apportioning ship emissions will be discussed in a future publication (454).

In general, all of the major particle types observed at the freeway site were also detected at the laboratory site. The similarities between the major particle types sampled by the standard ATOFMS instrument that was initially located at the upwind site (ATOFMS-2) and then moved to the freeway site were compared by taking the dot product of the top clusters detected at each site. All of the particle types detected at both sites had matching clusters with vigilance (similarity) factors of 0.85 and greater, meaning their mass spectral signatures were very similar to one another (a dot product of 1 indicates they are identical to one another). It is important to keep in mind that slight modifications due to uptake of organic carbon, ammonium, nitrate, and other secondary species will not have much of an effect on the comparison as the ART-2a weight vectors are sensitive to the most intense peaks in the spectra. The particle types deemed as

"unique" at both sites were mainly sea salt particles. This is because they had undergone less processing in general at the upwind site since it is closer to the ocean. The spectral modifications due to heterogeneous processing involve the loss of one peak from a relatively complex particle spectrum and the addition of another. For example, the uptake of NO_x or SO_x species on a sea salt particle will displace the chlorine on the particle which will result in the ATOFMS spectrum of the "aged" particle having different negative ion peaks than a fresh sea salt spectrum (455). Reducing the vigilance factor to 0.7 instead of 0.85 resulted in all particle types at the freeway site, including sea salt, matching the clusters at the upwind site. As would be expected, the rank order (based on the number of particles in each cluster) of the various types and their relative contributions to ambient PM was different at the two sites (i.e. there was more sea salt detected at the upwind site than at the freeway site, and more vehicle emissions detected at the freeway site than at the upwind site).

f. Data Analysis Used for Apportionment

The same method described in Chapter 4 for source apportionment using mass spectral source signatures was also used here (441). In short, several ATOFMS source characterization studies have been conducted for the purpose of obtaining unique mass spectral signatures for each source. The particle source library includes signatures for HDDV and LDV exhaust emissions, coal burning, biomass burning, meat cooking, sea salt, dust, and industrial emissions; as well as non-source specific signatures for aged elemental carbon (aged EC), aged organic carbon (aged OC), amines, NH_4-containing, vanadium-containing, EC particles, and PAH-containing particles. These source signatures are used as a "seed" database, where the mass spectra of particles from other studies can be compared to the seeds using a matching version of the ART-2a algorithm (456,457) (YAADA v1.20 – http://www.yaada.org). Each particle mass spectrum is compared to all the mass spectra (ART-2a weight matrices) in the source database one at a time taking the dot product between each. If the particle matches to a particular source seed above a designated dot product vigilance factor (VF) threshold, then the particle is assigned to that type. If the particle matches to two or more different source seeds above the VF, then it will be assigned to the one that provided the highest dot product. The dot product values range from 0 to 1 with a value of 1 indicating the particle types are identical. For this analysis, a relatively high VF of 0.85 was used.

The ART-2a matching method has shown that a significant fraction of the HDDV and LDV particle types acquired during dynamometer sampling are indeed representative of those produced near a roadway (37,441). The results in Chapter 4 also show that the particles detected near the freeway are readily matched to particles from the vehicle dynamometer studies (441). These previous results focused on particles sampled with the UF-ATOFMS sampling near the freeway in the 50 – 300 nm size range, because particles in this size regime denote freshly emitted particles that would have a greater probability of originating from vehicular traffic on the freeway. The previous results also focused mainly on matching LDV and HDDV particles, since those would be the most similar types and thus, the potentially hardest to distinguish from one another. For this paper, the particles from the UF-ATOFMS and the two standard ATOFMS instruments were subjected to the same mass spectral matching procedures. However, since there is such a large size range sampled by these instruments, particles are only matched to source

library particles of the same size range. Therefore, ultrafine particles (50 – 100 nm) are only matched to source particles in the same size range, and likewise for small accumulation mode particles (SAM) (100 – 140 nm), larger accumulation mode particles (LAM) (140 – 1000 nm), and supermicron particles (1000 – 3000 nm). Size segregated matching ensures that particle types from one source that may be similar to those of another source, but having very different particle size ranges, don't conflict with each other. The reason the accumulation mode was split into two libraries (for this study) was because of the regional background EC and vanadium types discussed earlier which were found to influence the apportionment of the accumulation mode particles with sizes above 140 nm (441). As previously mentioned, the source library currently contains signatures for HDDVs, LDVs, dust, sea salt, biomass, and meat cooking, along with non-source specific signatures for aged organic carbon, aged elemental carbon, amine containing particles, PAH's, ammonia rich particles, vanadium particles, and elemental carbon particles. The signatures for HDDVs and LDVs were primarily obtained from dynamometer studies. Additionally, some of the HDDV and LDV signatures were obtained directly from ambient sampling after such particles were found to match with the dynamometer seeds. Other sources, such as biomass, dust, sea salt, and meat cooking were obtained from both lab studies and previous ambient measurements. The seeds for aged organic carbon, aged elemental carbon, amine containing particles, PAH's, ammonia rich particles, vanadium particles, and elemental carbon particles were obtained directly from classified ambient data from several different studies. As mentioned earlier though, the vanadium and elemental carbon seeds (many of which were derived from this study) may actually be signatures for ship emissions (454).

g. Source Apportionment Using ART-2a

As described, ART-2a analysis was used to "match" ambient data to source seeds for the duration of the study. **Figure 102** shows the size resolved apportionment for the first part of the study (Jul. 24 to Aug. 3, 2004) and averaged over those days. In Chapter 4, the one hour temporal apportionment of LDV and HDDV particles is shown for this same time period (441). From those results, it was shown that for ultrafine

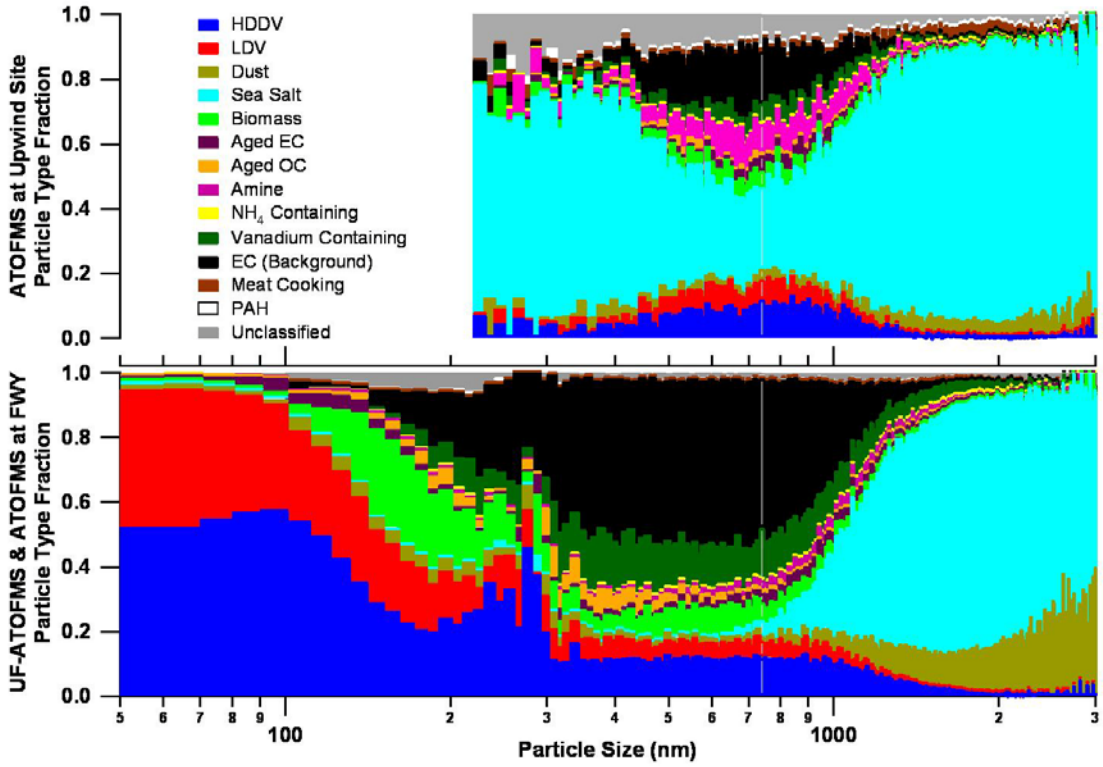

Figure 102: Size resolved source apportionment of the particles detected at the upwind (top) and freeway (bottom) sampling sites. Both plots are averages for ATOFMS data acquired from July 24 to Aug 3, 2004. In the bottom plot for the freeway site, the sizing region of overlap between the UF-ATOFMS and standard inlet ATOFMS is 200 – 300 nm.

particles, 37% of the particles were apportioned to LDVs and 58% to HDDVs. For accumulation mode particles (Da = 100 – 300 nm), 25% were LDV and 41% were HDDV. It was also shown that the trends of the apportioned particles tracked very well with LDV and HDDV vehicle counts. It is important to note that those results were only for particles detected with the UF-ATOFMS. Thus, when examining **Figure 102**, the ultrafine apportionment at the freeway site shows the same apportionment percentages as in Chapter 4. With the data from the standard ATOFMS being incorporated into the apportionment, size fraction trends through the region between 200 – 300 nm (where the two instruments overlap in particle size detection) for the HDDV apportionment is not as smooth due to the low number counts between 200 – 300 nm for both ATOFMS instruments. The trends of the other particle types in the 200 – 300 nm region are also not as smooth for the same reason as for the HDDV and LDV trends. The UF-ATOFMS was tuned to transmit ultrafine particles most effectively for this study by sampling ambient air drawn through a MOUDI with a 50% size cut at 100 nm to remove most of the particles larger than 200 nm, and thus making the transmission of particles above 200 nm relatively low (417). Likewise, the detection of particles below 300 nm by the standard inlet ATOFMS was low for this study. These size detection barriers for each instrument can be seen quite clearly in **Figure 99 (B,C)**. The relatively low detection efficiency of particles for each instrument between 200 and 300 nm during this study

accounts for the lack of a smooth transition for the particle types in the 200 – 300 nm size range.

As shown in **Figure 102**, ATOFMS allows for the determination of aerosol apportionment with very fine (10 nm) size resolution. This is important, because it can be seen that the fraction of particle types changes with size, especially above 100 nm. Above 100 nm, particles associated with biomass burning start to contribute to the ambient particles at the site, as well as particles apportioned to aged EC and aged OC. Most noticeable is the contribution from the EC (background) and vanadium-containing particle types starting around 140 nm (particularly for the EC background period). As discussed earlier, the regional background types were detected primarily at night, when local wind speeds were very low and when HYSPLIT back trajectories (**Figure 101**) come down the California coastline over Long Beach. These regional background types make up a major fraction of the particles from 200 – 1000 nm. The overall apportionment fractions stay relatively constant between 300 – 800 nm. Above 800 nm, sea salt particles start to contribute and become the dominant type above 1000 nm.

While seeds for non-aged and aged sources are included in the source signature library for non-vehicle sources, it should be noted that the sources are not currently being distinguished between aged and non-aged species to keep the apportionment simple. However, the majority of the particles from non-vehicle sources above 100 nm are coated with sulfate, nitrate, ammonium, as well as secondary organic aerosols (SOA) and that the amount of sec species increases with size based on ion intensities as one would expect.

When comparing the upwind site to the freeway site in **Figure 102**, one can see that sea salt particles dominated the detected particles at the upwind site. Interestingly, the particles apportioned to LDVs and HDDVs at the upwind site were primarily detected from 300 – 1000 nm. This observation could be an indication of growth of the vehicle particles as they were transported from the nearby roadway that is 200 meters upwind from this site. Unfortunately, there was not another UF-ATOFMS at the upwind site to see if there was an influence of vehicle emission on the UF mode. As shown in **Figure 98B**, there was very little contribution to the UF mode at the upwind site except when cooking emissions from a nearby cafeteria impacted the site. Over the 400 – 1000 nm size range, there is a greater fraction of amine-containing particles that do not match to any source library particles, a possible indication of aging occurring on the vehicle particles as they were transported to this site. A commonality between the freeway site and the upwind site is the detection of the regional background vanadium and EC particles over the same size range. As explained earlier, while the freeway site shows a higher contribution than the upwind site (40% of the total particles at the freeway versus 10% at the upwind site over the 140 – 1000 nm size range), the difference may be due to the topography of the area. The fact that the EC and vanadium particles are detected over the same size range is further evidence that these particles are part of a regional background as shown in **Figure 100**.

h. Size Resolved Source Apportionment Temporal Series

As previously mentioned, the initial time series of the ATOFMS source apportioned freeway particles using the mass spectral source library was presented in Chapter 4. In that chapter, the focus was on the apportionment of HDDV and LDV

emissions in the ultrafine size range. The particles that were not apportioned to HDDV and LDV were designated as "other" particles (441). For this current study, a mass spectral source signature library with additional clusters besides HDDV and LDV signatures was used. Therefore, many of the particles originally designated as "other" are now apportioned, as can be seen in size resolved apportionment results presented in **Figure 102**. **Figure 103 (A-D)** shows the time series of the ultrafine and accumulation mode apportionment results at the freeway site, similar to those shown in Chapter 4, but with less particles in the "other" category. **Figure 103** is ordered from the smallest size range at the top down to the largest size range at the bottom. Evident in this figure is the influence of non-vehicle particle types with the increase in particle size, just as **Figure 102** shows. Also, the time series shows that certain particle types, such as biomass, are more prevalent on the weekends than the weekdays. Another interesting feature is the Aged OC class spikes on July 27, 2004 in the UF-ATOFMS 140 – 300 nm size range and the ATOFMS 200 – 1000 nm size range. This spike can also be seen in the ATOFMS number concentration plot in **Figure 99**, occurring at the same time across the same size ranges. The particles that matched to the Aged OC signatures during this time are fairly unique, as they only spiked with the two instruments on this one day during the study. One of the main points of **Figure 103** is to show that even near a freeway, one is not just being exposed to freeway aerosols. During times with a high regional background influence, the freeway related PM above 100 nm represented a relatively small fraction of the overall concentrations.

The time series of the ATOFMS (300 – 1000 nm) particle fractions in **Figure 103** compliment **Figure 100** & **Figure 102**. As shown in **Figure 103**, the EC background type dominates the particles between 300 and 1000 nm, with a strong contribution from the vanadium particles as well. The time series in **Figure 100** shows that the EC & vanadium made a large contribution to the particle concentrations from 7/24 – 7/27. This is also quite evident in **Figure 103** for the ATOFMS 300 – 1000 nm time series.

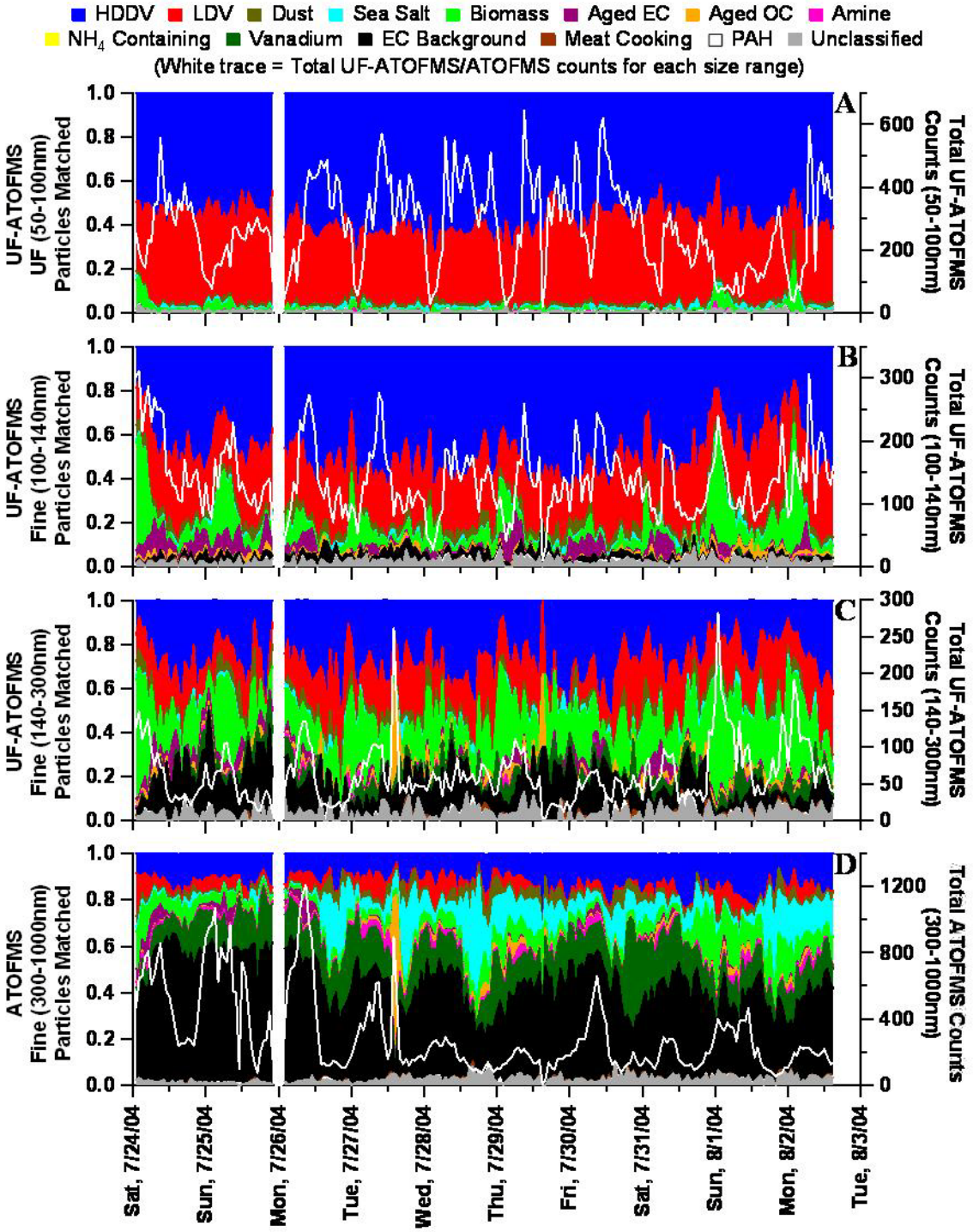

Figure 103: Time series of the size segregated source apportionment fractions for the freeway site ultrafine and accumulation mode particles detected with the UF-ATOFMS and ATOFMS.

One should note that all results presented here are based on a relatively simplistic univariate data analysis approach using ART-2a. However, even with this simplistic approach, the results demonstrate how single particle data can be used to apportion source contributions to ambient data. Particle aging, coating, agglomeration, and water uptake will play important roles in affecting particle source apportionment in other studies using this source library technique. These changes will, undoubtedly, make matching to source signatures more challenging, particularly at locations further from the source. Many of the sources, such as biomass, sea salt, and dust are readily distinguishable whether or not the particles are aged. The biggest challenge with aging will be with differentiating LDV and HDDV exhaust particles from one another. However, there are unique features to the HDDV and LDV sources that should make matching consistent, whether the particles have aged or not. One of the most important factors is that HDDV particles tend to have more calcium and phosphate associated with them in an elemental carbon/calcium type particle (EC-Ca) (37,419). LDV particles have much less calcium and/or phosphate associated with them, but do produce elemental carbon particles in the UF size mode (418). These kinds of distinctions could be used to identify HDDV and LDV particles in highly aged environments that do not match to the source seeds.

One of the ultimate goals of this study is to eventually compare single particle source apportionment with impactor filter samples acquired during this study. Single particle measurements hopefully can distinguish between unique vehicle source signatures superimposed on a high ambient background concentrations that may not be apparent in MOUDI mass concentrations where only slight changes are due to vehicle emissions (at least for the accumulation mode). Also, once the data are available, the source percentage predictions made with ART-2a on the ATOFMS data will be compared with organic tracer MOUDI and impactor based method results from this study obtained by the Kleeman research group from UC-Davis. Additionally, future analysis using different clustering algorithms, such as Hierarchical clustering and Positive Matrix Factorization, will be used in comparison to the results found in this chapter and Chapter 4 (441).

iv. Acknowledgements

The authors thank Dan Cayan and Alex Revchuk of the Scripps Institution of Oceanography (SIO) at UCSD for setting up the micro-meteorological stations and providing their data for this study. We also thank UCSD and their facilities management for all their cooperation and help with setting up power to the freeway site. Lastly, we thank Michael Kleeman and Michael Robert from UC-Davis for their collaboration with this study. The HYSPLIT transport and dispersion model used in this publication was provided by the NOAA Air Resources Laboratory (ARL). Funding for this study was provided by the California Air Resources Board (CARB) (Contract 04-336).